RKB Optimized Engineering Solution for Concrete Mixer Gearbox

Alberto BARILI, Ciprian RADU, Catalin DANAILA, Spiridon CRETU
RKB Bearing Industries – Department of Advanced Software Engineering

Abstract: *In an increasingly competitive sector, the RKB Group, with Executive Headquarters and Technological Center in Balerna (Switzerland), has decided heavy investments in Research & Development to efficiently satisfy the requirements of the power transmission industry, which is becoming more and more demanding in terms of performance and cost-effectiveness. The present article illustrates the steps taken by the RKB Group to develop a customized rolling bearing in co-engineering with a leading European manufacturer of gearboxes for concrete mixers. As usual, the whole engineering process was supported by the use of in-house developed software systems (MTDS, RRLC and NON-HERTZ), 2D and 3D CAD tools, and FEM analysis systems. The WOR bearings designed for this special project were finally manufactured by RKB using the latest machining technology and the best raw materials and heat treatments.*
Key words: *wide outer ring bearing, concrete mixer, contact pressure, optimization, reaction force, von Mises stress*

1 INTRODUCTION

Concrete mixer gearboxes are part of transit mixing trucks and transmit the rotational movement from a hydraulic motor to the drum. As the concrete payloads are charged into the drum, also while traveling to the work site, the drum is rotating and continuously mixes the load in order to prepare it and avoid its consolidation. During the transport, the gearbox rotates the drum in one direction (charge direction) and by using internal helical drum fins the concrete load is kept away from the discharge opening. When discharging, the direction of rotation is reversed.

The latest generation of gearboxes features innovative solutions that increase reliability, eliminate limitations and ineffectiveness from the old designs, and reduce costs and maintenance. With the purpose of driving the drum and carrying the torque forces and a part of the drum weight, the concrete mixer gearbox represents the key element of the application. The main bearing that supports the load transmitted from the drum has a crucial role in achieving maximum performance and reliability. For this reason, the design of the bearing was the main focus of the whole engineering process.

2 APPLICATION DESCRIPTION

The exploded arrangement in Fig. 1 highlights the main components of the double stage planetary gear speed reducer through which a hydraulic motor drives the mixing drum.

The hydraulic motor transfers the rotational movement to the input pinion shaft 1, that drives the 1st stage planetary gear 3, with deep groove ball bearings 4 that rotate the pinion shaft 6 of the 2nd stage planetary gear 7 sustained by SRB 8 inside it. The 2nd stage planetary carrier 9 couples the crown gear 10 that transmits the torque forces to the output flange 14, also absorbing misalignment. The main SRB WOR design 11 is protected against contaminated environment by the seal 13. The gearbox has to be mounted on a rigid, free distortion support. If the mounting is not rigid, it can damage the internal gears, the seals, and finally the bearings.

The configuration of this design is engineered to withstand the application requisite operating conditions in a safe and reliable way. This objective is attained with described gearboxes, which drive and pivotally support the mixing drum, compensating the motion between the mixing drum and the main bearing case.

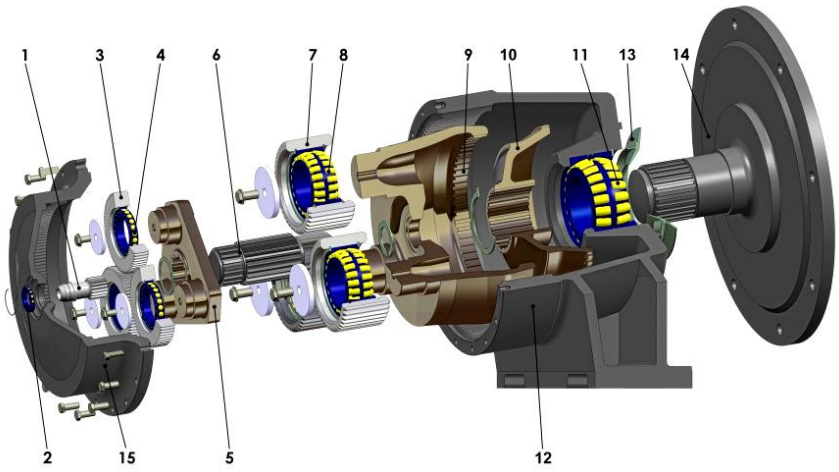

No.	Component
1	Input pinion shaft
2	RKB deep groove ball bearing
3	1st stage planetary gear
4	RKB deep groove ball bearing
5	1st stage planetary carrier
6	Pinion shaft
7	2nd stage planetary gear
8	RKB spherical roller bearing (SRB)
9	2nd stage planetary carrier
10	Convex gear
11	Main RKB SRB WOR design bearing
12	Main housing
13	Seal
14	Output flange
15	Rear cover

Fig. 1 – Two-stage planetary gearbox explosion

3 BEARING SELECTION

Due to the drum installation angle and its applied load, the main bearing that supports the application needs to be able to absorb heavy radial and axial forces combined with important misalignment induced by the drum. This condition directly leads to a customized solution for spherical roller bearing design.

In general, distinct heavy engineering applications incorporating spherical roller bearings may need different bearing configurations, such as the CA, ECA, CC, MA and MB, showed in Fig. 1, just to mention the most common. The differences primarily lie in the design of the inner ring and cage. Because of the technical characteristics of the present application, such as low rotational speed, high thrust load, moderate shocks and increased misalignment, the bearing design must feature a cage made of two pieces that enable the two rows of reinforced rollers to move independently from each other.

Fig. 1 – Different RKB spherical roller bearing designs

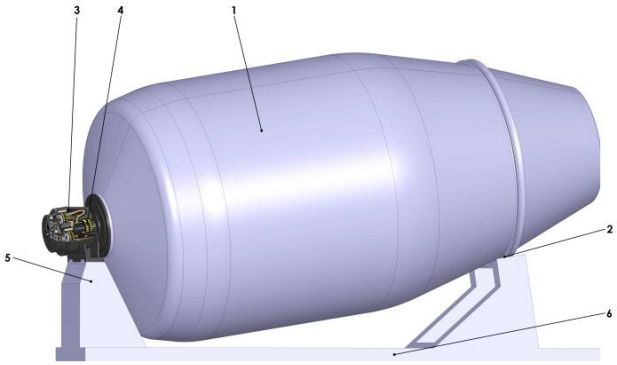

Fig. 2 – *Mixing drum assembly*

The mixing drum is supported on the one hand by two guiding rollers 2 and on the other hand by the drive 3, Fig. 2. Because of its loaded weight and installation angle, the main bearing 4 must be capable of accommodating higher

values of misalignment than standard spherical roller bearings. Moreover, if the transit vehicle travels on uneven terrain, the main bearing 4 must be able to transfer the mixing drum weight 1 to the bearing bracket 5 that is connected to the vehicle frame 6. In such extreme conditions, the vehicle frame deforms, leading to a relative motion between the bearing bracket and the mixing drum, which induces shocks in the main bearing. In order to protect the main bearing from excessive shocks during operation, the bearing bracket should be mounted on shock absorbers.

4 BEARING DESIGNS

In order to accommodate higher values of misalignment the bearing outer ring is redesigned and optimized, bringing about an increased outer ring width. The main differences between the outer rings of normal design spherical roller bearings and those of special WOR design are pointed out in Fig. 4. The resulting optimized surface geometry of the outer ring allows the bearing to accommodate higher angular misalignment than standard spherical roller bearing, maintaining the bearing performances. In addition to heavy radial loads, this bearing design supports heavy axial loads and demanding misalignments, making it irreplaceable for concrete mixer applications. WOR bearing series is a special design, having two separate outer raceways connected with a clamping ring that facilitates mounting and dismounting.

a) b)

Fig. 4 – Differences in SRB executions: a) standard design; b) WOR design

Separate cage, reinforced rollers and increased outer ring width are only a few of the design features that made the bearing suitable for the above mentioned application.

Since the main bearing is a key element in the gearbox running performances, the attention is focused on designing the proper bearing that will satisfy the application requirements. Based on the main boundary dimensions, the load capacities and the application particularities, three bearing designs (Fig. 3) have been developed and involved in the current study: 24122 WOR82A, 24122 WOR82, and 24122 WOR82AA. A 3D computer analysis has been further carried out to validate the bearing design for the concrete mixer gearbox.

All three designs have been configured with separate brass or steel cages. Compared to the machined brass cage design (Fig. 3 b) the window-type design (Fig. 3 a, c) incorporates more rollers for the same main boundary dimensions, affecting the load rating capacities of the bearing.

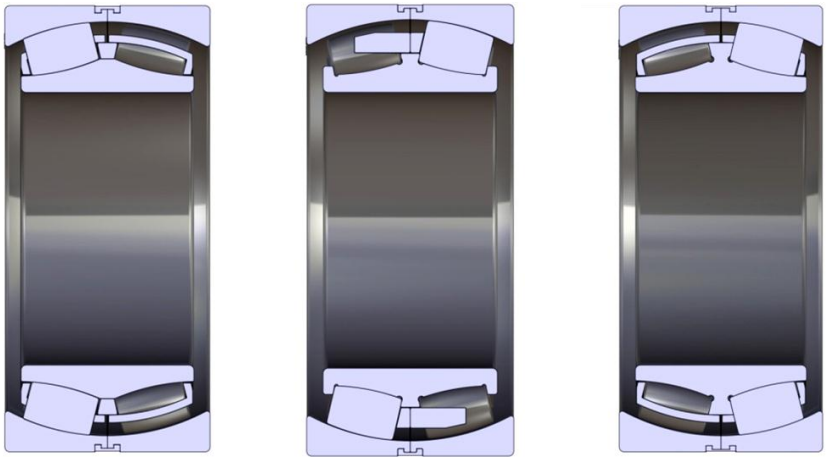

a) b) c)

Fig. 3 – 3D models of different RKB SRB designs: a) 24122 WOR82A; b) 24122 WOR82; c) 24122 WOR82AA

RKB spherical roller bearing 24122 WOR82A design (Fig. 3 a) is a bearing with symmetrical rollers, flangeless inner ring, a non-integral guide ring between the two rows of rollers centered on the inner ring and pressed steel window-type cages for each row of rollers. The two-piece cage enables the two rows of rollers to move independently from each other, which is beneficial in applications with extreme thrust loading. Moreover, the non-integral ring centered on the inner ring acts as a guiding ring for the rollers, that are correctly driven into the loaded zone. The separate cage keeps the rotating rollers in a stable condition, allowing for minimum temperature rise and improved operating time. This design permits to obtain a significantly reduced cage section because the bridge is supported on both sides. In addition, this type of cage eliminates the need for the inner ring retaining flanges and allows for more and larger rollers, which remarkably increases the load carrying capacity.

RKB 24122 WOR82 design (Fig. 3 b) is a bearing with asymmetrical rollers, a two-piece machined brass cage guided on the fixed central inner ring rib and retaining flanges on the inner ring. In case of asymmetrical roller design, the rollers are pushed into the central fixed rib. This enables to attain smoother running of bearings, reducing sliding friction and heat generation, which is extremely beneficial in low speed applications, and providing longer lubricant life. If the application is subjected to high thrust loads and if the magnitude of the shock loads is pronounced, additional load and higher internal friction on the rib will be generated.

RKB 24122 WOR82AA design (Fig. 3 c) is a bearing with symmetrical rollers, a two-piece pressed steel window-type cage for each row of rollers guided on the inner ring central fixed reinforced rib. This design encompasses the previous 24122 WOR82 design featuring an increased numbers of rollers and length for a greater load rating. The central fixed inner ring rib is reinforced to sustain additional load and friction.

In addition to this special design, a high cleanliness steel and RKB Isothermal Bainitic Hardening Treatment (HB) for the inner ring come to reinforce the bearing strength and resistance to high tensile interference fits and high shock loads, reducing at the same time the occurrence of ring cracking.

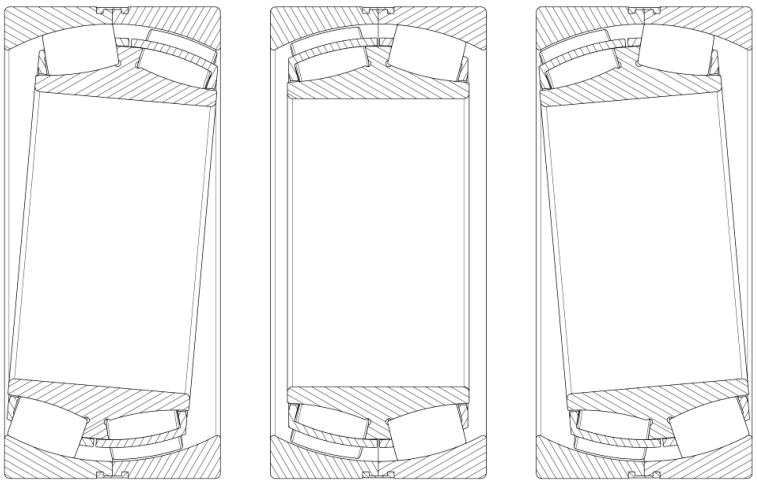

a) b) c)

Fig. 6 – Maximum permissible misalignment of RKB SRB WOR design: a) -6°; b) 0°; c) +6°

Due to their design and macro-geometry, all of the three bearing designs are able to withstand the application particularities, but care has to be taken on the magnitude of axial loads applied combined with big shocks and variable misalignment. Under extreme operating conditions the misalignment value between the inner ring and outer ring is variable and consequently additional sliding motions will be generated in rollers-raceways contacts as well as rollers-cage contacts. These supplementary motions occur in a poor lubrication regime that leads to increased friction and temperature, causing abrasive and adhesive wear and finally determining bearing failure. Therefore, it is highly recommended that the misalignment of the inner ring with respect to outer ring not exceed the designed, permissible angular misalignment value (Fig. 6). According to the application operating conditions, the right choice of lubricant type and quality is fundamental (suitable viscosity and cleanliness) to achieve the necessary elasto-hydrodynamic film thickness.

For any roller bearing, the dynamic radial load rating C_r appears as a function of the number of rollers Z, the effective length of rollers L_{we} and roller diameter D_{we}. Consequently, the varied cage designs act as endeavors to improve as much as possible the values of these parameters (Fig. 4 a). Moreover, by changing the nominal contact angle with the inner ring designs (Fig. 4 b), one obtains various internal geometry parameters that lead to a better accommodation for axial loads and differences in bearing load rating capacities. The load rating capacities of the three bearings were calculated with RKB MTDS software based on the properties and characteristics of the parts.

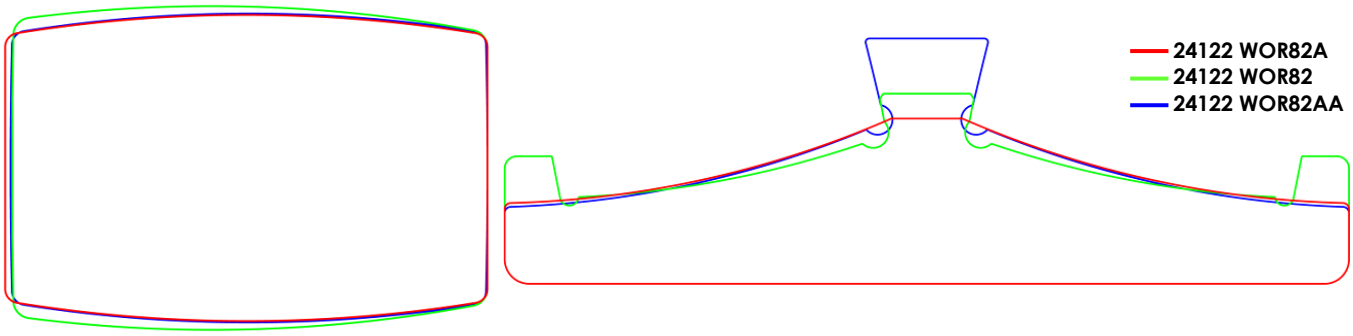

a) b)

Fig. 4 – SRB WOR design differences for: a) rollers; b) inner rings

The RKB MTDS software (Fig. 5 a) offers consistent background information on the calculation of the bearing static and dynamic load ratings according to the latest versions of ISO 76 and ISO 281. The differences in static and dynamic load ratings, due to the internal macro-geometry particularities of the three bearings, are normalized and shown in Fig. 5 b.

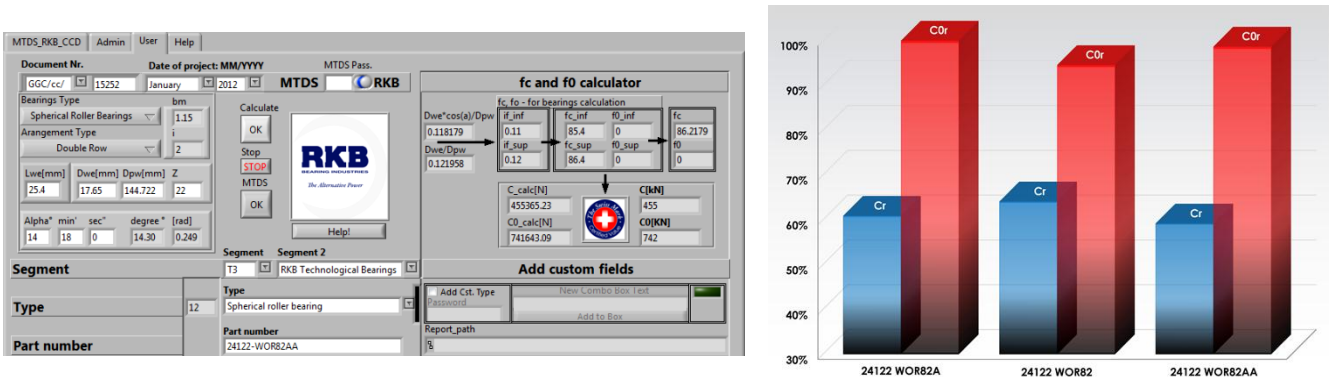

a) b)

Fig. 5 – RKB MTDS software: a) user interface; b) C_r and C_{0r} results of 24122 WOR82A, 24122 WOR82, and 24122 WOR82AA designs

5 APPLICATION OPERATING CONDITIONS

According to the application design and requirements, the operating conditions of the mixer can be different. On the other hand they have to be found within the limits established by the ASTM Specification for Ready Mixed Concrete or other similar authorities. Depending on the concrete requirements to obtain the requested performances on the working site, the truck variable operating conditions are to be set. Since the concrete is an alterable product exposed to possible loss of properties as a consequence of certain factors (e.g. temperature and delivery time), the proper proportioning of the selected concrete ingredients along with a correct mixing cycle are to be established by the concrete producer based on its previous experience. Depending on the mixture type and drum capacity, raw materials (cement, sand, water, aggregates and other materials) are simultaneously introduced in the drum, at medium to high speed. Once the charging procedure is completed, the mixing method is initiated. There are several required operating procedures for the concrete to be properly mixed and reach the desired properties such as strength, durability and, workability.

- In the yard. This practice imposes a concrete mixing for about 50 revolutions at high speed between 10-15 rpm. After completing this stage, concrete is agitated at a lower speed, which is 2-4 rpm, up to the moment when it reaches the work site.
- In transit. The concrete is mixed for about 70 revolutions at medium speed between 8-10 rpm while driving to the work site, then the speed is decreased.
- In work site. During the concrete transportation to the work site, it is maintained at agitating speed, whereas, at the moment it is brought to the work site, speed is increased to 18-20 rpm, for about 70-100 revolutions.

If, for any reason, the mixed truck operator decides to add water after the concrete has been mixed, additional 30 revolutions at maximum speed should be performed. Depending on the mixture type, job conditions and drum size, the mixture is discharged at a drum speed of 10-14 rpm. Since the mixer is loaded and water was added to the cement, up to the time when the discharging sequence is accomplished, the revolution counter shouldn't record more than 350 revolutions or 90 minutes.

The lifetime of the drum is limited by the inner helicoidal fins strength and shape. Therefore selecting the proper working cycle is crucial in the concrete performance and will be in time reflected in practical and economic efficiency.

Table 1 – Concrete mixer estimated operating conditions and cycles

Mixer operating conditions	Time (min)	Speed (rpm)	Revolutions
Loading at plant	3	20	60
Mixing	6	18	108
Travel time	30	4	120
Discharge	3	14	42
	Average revolutions		330
Daily cycle (trips per day)		4	
Revolutions per day		1320	
Revolutions per year (200 operating days)		264000	
Revolutions per drum life (5.6 years)		1478400	

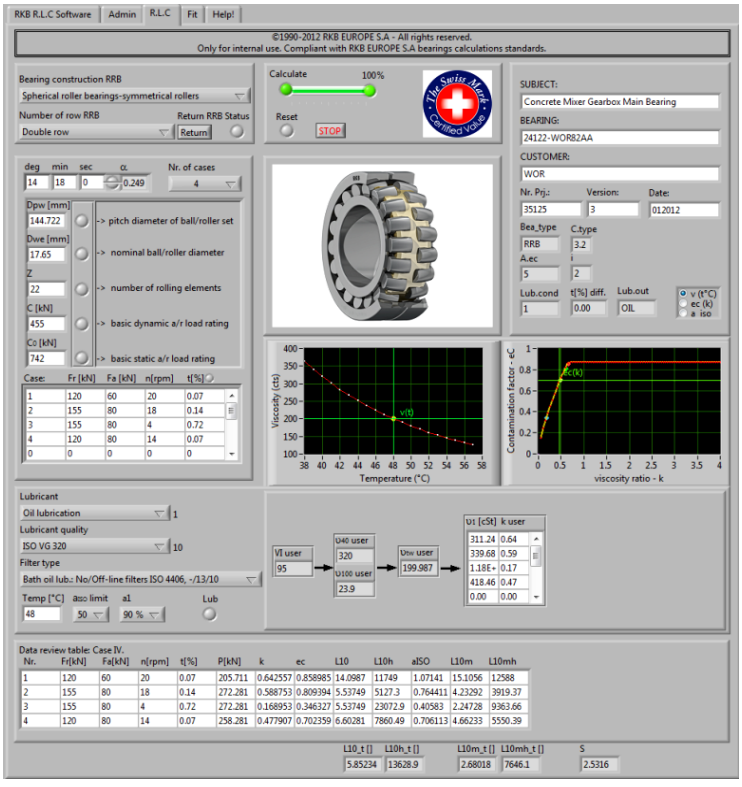

a)

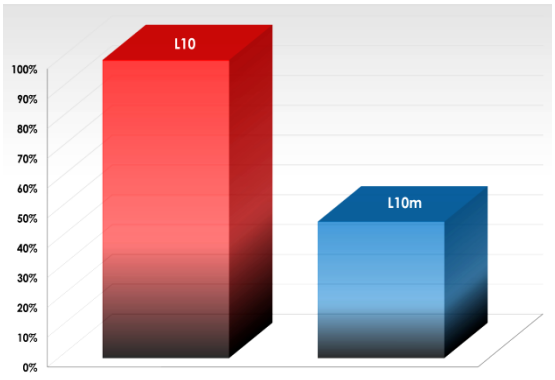

b)

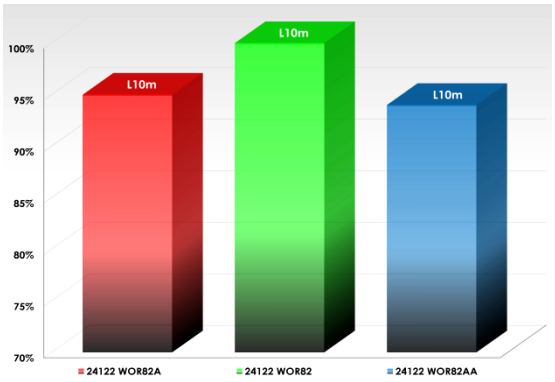

c)

Fig. 6 – RKB Rating Life Calculations software: a) user interface; b) difference between the basic rating life L_{10} and modified rating life L_{10m} of 24122 WOR82AA design; c) L_{10m} results of 24122 WOR82A, 24122 WOR82, and 24122 WOR82AA designs

The drum weight and part of the weight generated by the concrete volume act directly on the drive main bearing as a combined radial and axial force. The variable operating conditions imposed by the drum mixing cycles have a direct influence on the main bearing life. In order to evaluate the bearing life it is necessary to reduce the described working conditions to a limited number of cases (Table 1). In this case, each different load level from the variable loads is accumulated and reduced to a constant load. These duty intervals are averaged in given percentages of time fractions, speed intervals, temperature differences, lubrication conditions and levels of contamination.

To calculate the bearing life under the above mentioned percentages and considering the applied loads, variable speed, operating temperature, lubricant influence and the requirements regarding service life, reliability and safety index, RKB RRLC in-house developed patented software system was used. The modified rating life L_{10m} (Fig. 6 c) calculated with RRLC software (Fig. 6 a), for all of the three bearings, taking into account the application specifications, satisfies the required design life of the complete gearbox-drum system. As shown in Fig. 6 b, the difference between the basic rating life L_{10} and the modified rating life L_{10m} of the 24122 WOR82AA design is considerable. The modified rating life decreases because the bearing is subjected to low operating speeds, using the same lubricant quality as for the gear of the input shaft that runs at high rotational speed. In this case, extreme pressure additives will be used to provide boundary or mixed lubrication and anti-scuffing protection. Also, according to the gearbox manufacturer, the first change of the lubricant is to be performed at 100 operating hours so as to remove any metal particles that can damage the bearings. The following lubricant change must be made after every 1000 operating hours or within one year.

6 FINITE ELEMENT AND SEMI-ANALYTICAL SIMULATIONS

Two groups of numerical methods are commonly involved in solving the non-Hertzian contact problems: the finite element method (FEM) and the semi-analytical method (SAM). The FEM can simulate complex material behaviors and is today's most used numerical method to solve problems in solid mechanics. However, it needs an extremely fine mesh of the volume surrounding the contact zone, which means a major increase in computing time and costs. Moreover, to diminish the computation time, providing a quicker response to customer requests, SAM needs only a very small contact region to be involved in the numerical analysis. A specific SAM and the corresponding software tool, called NON-HERTZ, have been developed in the RKB Engineering and Research Department to analyze the non-Hertzian contacts running in the elastic-plastic range and the depth distributions of von Mises equivalent stresses.

RKB engineers subjected the three different bearing designs to FEM and SAM analysis to achieve maximum performance and reliability. With a numerical approach, all the analyzed bearing designs (24122 WOR82A, 24122 WOR82, and 24122 WOR82AA) have been evaluated in terms of reaction forces, von Mises equivalent stresses, and contact pressure distributions. For this purpose, several static structural analyses have been performed by using Ansys 13, the leading finite element software tool. In particular, the following steps have been taken:

- Pre-processing of the models starting from the importing of their 3D geometries from Catia V5R19 to Ansys Design Modeler module to the final settings before launching the analysis in Ansys Mechanical module.
- Processing of the input data executed by the direct solver of Ansys Mechanical module to reach the static equilibrium state solution.
- Post-processing of the results obtained in Ansys Mechanical module.

6.1 Pre-Processing Stage

The following procedures have been closely applied to each of the three spherical roller bearing designs. In particular the application using 24122 WOR82AA design will be analyzed in detail. Since only the bearing mounted on the output shaft is the subject of our study, only a part of the 3D model of the concrete mixer gearbox has been used for the finite element analysis. The following 3D components have been used:

- Main RKB spherical roller bearing WOR design,
- Shaft and output flange,
- A part of the main housing,
- Convex gear.

The Catia 3D model of the concrete mixer gearbox, containing the 24122 WOR82AA design, has been imported in Ansys Design Modeler module. Operations such as merging of surfaces and edges, geometry simplification, and body splitting have been performed in order to obtain a valid model for a correct analysis. Moreover, in order to simulate the geometry and operating characteristics of the mixing drum, a beam structure with tubular cross-section has been used (Fig. 7). The remaining pre-processing operations have been performed in Ansys Mechanical module.

For each deformable body an elastic material behavior has been assigned, meaning that to a single admissible stress value corresponds only one strain value. The plastic material behavior was not purposely assigned for this evaluation in order to decrease the analysis computational time. The mechanical properties of the steel assigned to the model components are presented in Table 2. Steel has been used as a material for all metallic components,

while rubber has been selected for the clamping ring between outer ring split parts. Only the cages have been modeled as rigid or undeformable bodies, since their behavior is not part of the present evaluation.

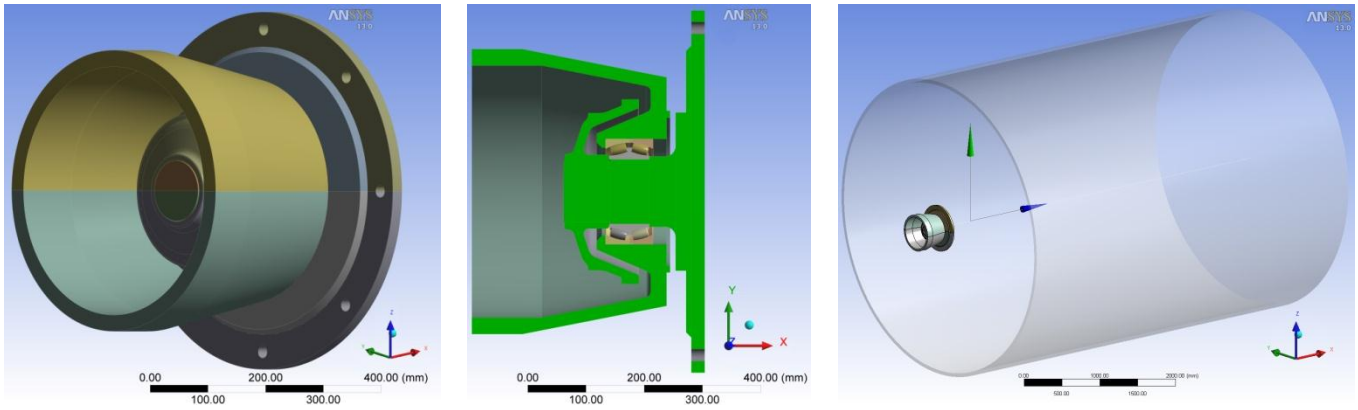

a) b) c)

Fig. 7 – Concrete mixer gearbox geometry preparation: a) studied assembly; b) assembly section; c) drum simplified model (beam structure)

Table 2 – Material mechanical properties

Symbol	Parameter	Material	MU
		Steel	
		Value	
υ	Poisson's ratio	0.30	-
E	Young's modulus	$2.10 \cdot 10^5$	MPa
K	Bulk modulus	$1.75 \cdot 10^5$	MPa
G	Shear modulus	$0.81 \cdot 10^5$	MPa
ρ	Density	$7.80 \cdot 10^3$	kg/m^3

The next step in the pre-processing stage involved the definition of the contact between components. The non-linear contact problem is a complex mechanical phenomenon arising from the interdependency of the machinery parts.

The analyzed model comprises many interacting parts. Every interaction generates a mechanical contact that has to be included in the analysis as it is in the real operation of the concrete mixer gearbox. For the components in contact, where the relative sliding is allowed, a frictional contact has been assigned with a pure penalty algorithm. For the others, where no relative motion is permitted, a bonded contact with pure penalty or MPC algorithms has been assigned.

The applied settings for each contact comprise the surfaces being in contact (the contact surface in red color and the target surface in blue color, Fig. 8), the coefficient of friction between two surfaces in contact (if any), the contact algorithm, and the normal stiffness factor (to control the penetration between bodies in contact).

For the frictional contact with pure penalty algorithm, normal and tangential contact stiffnesses are automatically calculated by the program based on the geometry and mesh density. The normal stiffness has a paramount importance in achieving an accurate solution, since the penetration between two surfaces in contact depends on it. Although higher stiffness values decrease the amount of penetration, it is possible to obtain an ill-conditioning global stiffness matrix creating difficulties in getting the final solution. On the contrary, lower stiffness values can lead to an improper solution characterized by a high amount of penetration. Considering these assumptions, many simulations have been performed in order to find the highest normal stiffness and ensure the highest quality of the results.

To simplify the situation, but without introducing errors in the final solution, bonded contacts with pure penalty algorithm have been considered between both roller rows and cages. Even if the contacts are bonded, the pure penalty algorithm, with a studied normal stiffness factor, will permit the rollers to have a relative small movement inside cage pockets, adjusted to be equal to the admissible play. The contacts between rollers and inner and outer

ring raceways, where the rolling motion exists, have been simulated as frictional contacts. In this way, a rolling coefficient of friction and a pure penalty algorithm have been adopted. Further on, for the contacts between roller side faces and inner ring integrated flange faces, the same frictional contacts have been used but with a sliding coefficient of friction.

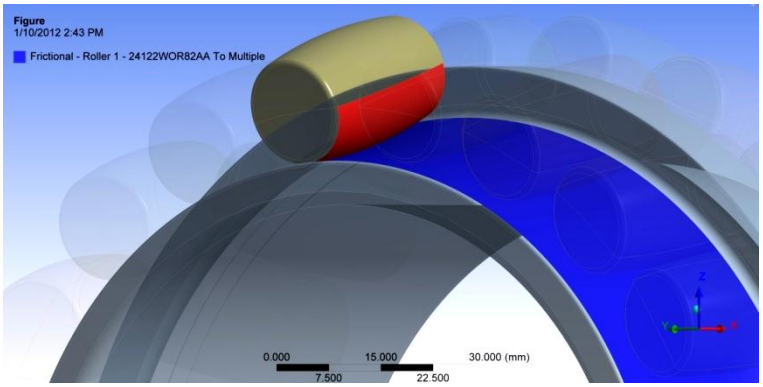

Fig. 8 – Contact and target surfaces

As for the contacts between inner ring bore and shaft and outer ring outer surface and main housing, both of them have been modeled as frictional contacts with pure penalty algorithm. For inner ring bore and main shaft contact, an interference fit has been simulated to introduce the typical stress field with radial compressive stress for inner ring and shaft, a tangential traction stress for inner ring, and a tangential compressive stress for shaft.

After implementing the contact definitions for the rolling bearing components, other connections have been established for the rest of the model components. To simulate the actions of the bolts, which connect the mixing drum and output flange, the beam structure with tubular cross-section representing the drum has been connected with the flange by using a rigid joint. As Fig. 9 shows, a coordinate system has been created in the center of the flange to relate all the degrees of freedom (three translations and three rotations) of the beam edge with the holes of the drum. To let both cages move according to the inner ring, the same type of rigid joint has been applied, but having as a reference a coordinate system located in the bearing center of rotation (Fig. 9 b).

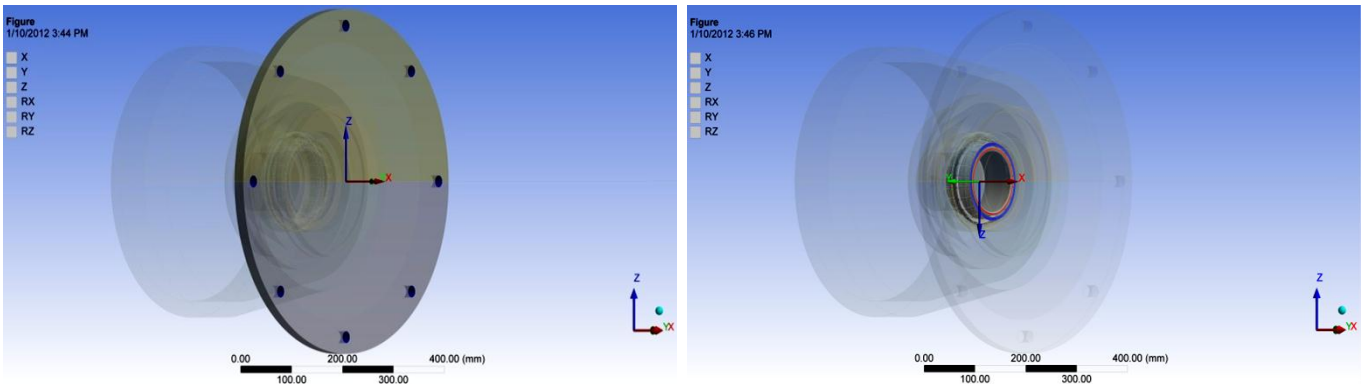

a) *b)*

Fig. 9 – Definition of joints between: a) drum and output flange; b) cage and inner ring

One of the most important steps in the pre-processing was the discretization (meshing) of the geometrical model. The entire geometrical model has been discretized into disjointed components with simple geometry called finite elements, characterized by distinguishing points named nodes.

A particular attention has been paid to the meshing method, involving a set of tests to determine which is the minimal dimension and density of the elements that does not revise the final results.

Initially, the discretization of the geometrical model in finite elements has been performed automatically with the default settings of the Ansys Mechanical module. As is evident in Fig. 10 a, the finite elements are not regular and are distorted in the case of rollers. Moreover, all of the bearing components present a low density mesh that may affect the accuracy of the solution, especially in the contact regions where the contact area between rollers and inner and outer ring raceways is a point. Thus, further mesh operations (Fig. 10 b) have been performed in order to obtain

a uniform element distribution with a high density population only in the bearing interest areas. For the rest of the components, meaning the main shaft with the output flange, a part of the main housing, the convex gear and the drum, a coarse mesh has been used to reduce the total number of elements, speeding up the analysis solving time.

To prepare and optimize the model for the meshing process, the bearing geometry has been previously sliced in many regions in the Ansys Design Modeler module. All the model components have been meshed as deformable bodies, except for the cages which have been considered rigid bodies. For each deformable body, different 3D elements have been assigned, while in the contact areas of the rigid bodies only 2D elements have been used. The imposed 3D structural elements are the 2-node beam element for the drum and the 20-node brick element for all the remaining deformable bodies. The assigned 2D structural element is represented by the 8-node quadrilateral shape element. Due to the complexity of the model geometry, other degenerated meshing elements have been used such as: 10-node tetrahedron, 13-node pyramid, 15-node wedge, and 6-node triangle elements.

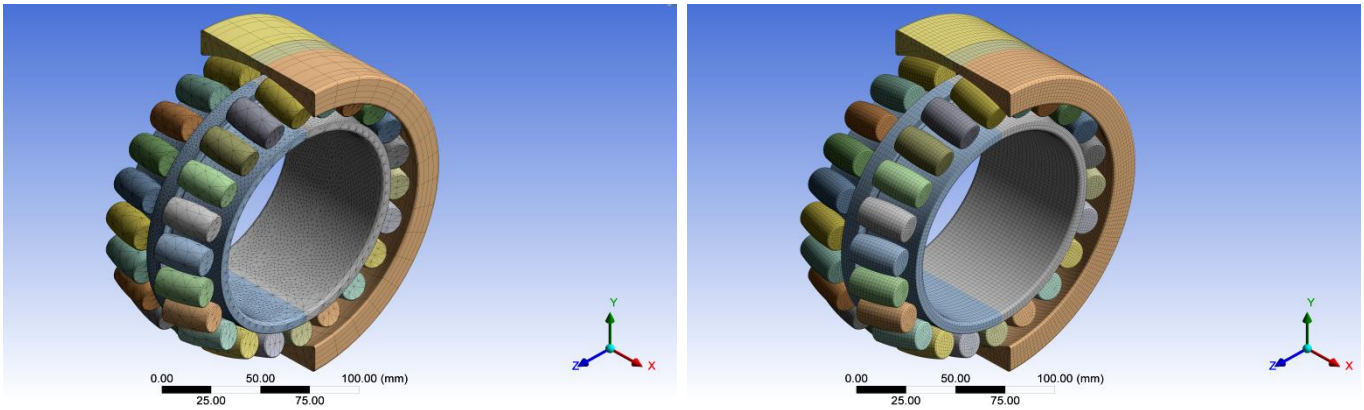

a) b)

Fig. 10 – Geometrical model discretization: a) automatic; b) optimized

The boundary conditions will be taken into consideration later in the present article. They are of a great importance for the static structural analysis because, under different kinds of boundary conditions, the structure behaves in different ways. In order to represent schematically the imposed boundary conditions and the applied force, the entire model was reduced to a hinged support, a beam, and a roller support (Fig. 11). These schemes have been the main guidelines to constrain the model with Ansys Mechanical module bringing it closer to reality as much as possible.

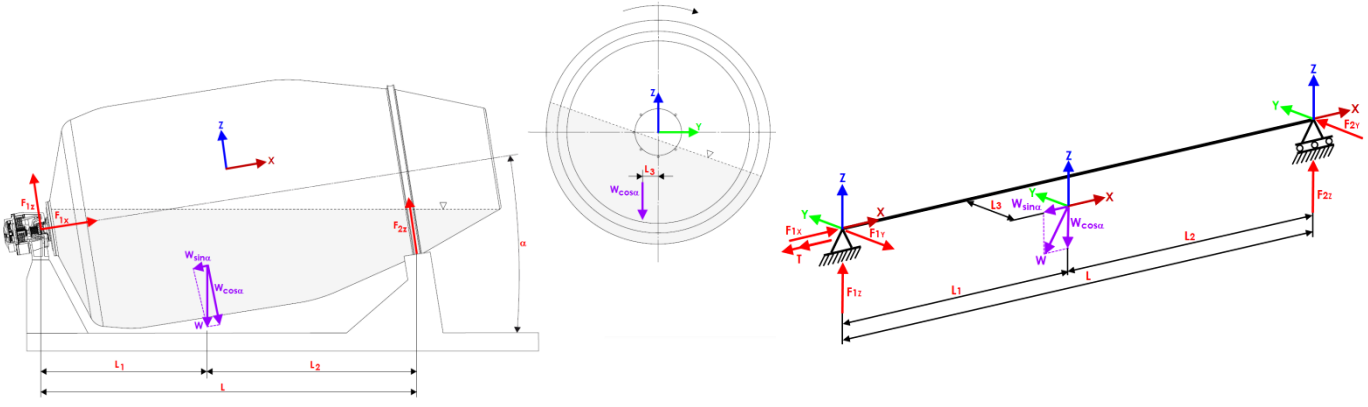

a) b)

Fig. 11 – Force representation on: a) entire model; b) simplified model

The hinged support is represented by the main spherical rolling bearing inside the concrete mixer gearbox housing. This support has been modeled to constrain the displacements of the drum along the axial and radial directions (X, Y and Z axis). The reaction forces of the hinged support are generated by the concrete mixer gearbox main housing, which in turn has been constrained with a fixed support.

To maintain the structure in isostatic state, the roller support, representing the second support of the drum, has been modeled to constrain only the radial displacements of the drum, leaving it free to displace along the axial

direction. The total load applied to the model compounds the weight generated by the maximum volume of concrete inside the drum and the drum weight.

In Fig. 11 a, the application point of the total load is out of the drum median plane and for a better understanding two views in different planes are given (Z-X and Z-Y planes). Due to the fact that the drum axis of rotation is inclined with α angle, with respect to horizontal axis, the total load affects the structure also with an axial component, taken entirely by the hinged support. The total load (*W*) has been projected, on the Z-X plane, along Z and X directions taking into account the inclination angle of the drum. The resulting components produce reactions called F_{1x}, F_{1z} on the hinged support and F_{2z} on the roller support.

The present study has been conducted in static conditions, but a dynamic effect has been implemented to the model. As can be seen from Fig. 11, the total load acts in a parallel plane with respect to the median plane of the drum, displaced with L_3 length, generating a bending effect on the X-Y plane and a resistant torque.

The composed weight component on Z direction transmits a resistant torque on the drum that, in static conditions, has to be balanced by the hydraulic engine coupled with the gearbox. To balance the resistant torque, generated by the concrete weight, a boundary condition has been applied to the convex gear, by blocking the rotation around its X axis. Two reaction forces named F_{1y} and F_{2y} (Fig. 11 b), acting in the X-Y plane, are generated by the composed weight component on X direction, eccentric by L_3 length with respect to the axis of the drum.

6.2 Processing Stage

Once all the boundary conditions have been implemented and the analysis settings established, the processing stage starts. Due to the frictional contacts, the simulation is governed by non-linear equations. The solution of the non-linear analysis has been determined by the Newton-Raphson method, in which the total load has been incrementally applied (ramped effect, Fig. 12).

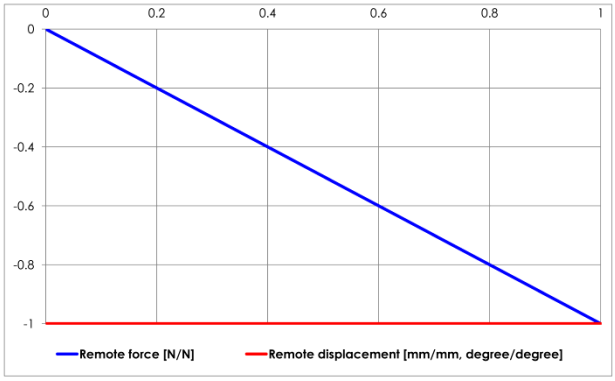

Fig. 12 – Incremental effect of the applied load

In Fig. 12, on the horizontal axis, the total time required by the solver to apply the total load magnitude, represented on the vertical axis as a normalized value, is shown. At the beginning of the analysis, the force (blue line) applied to the model is equal to 0 but it reaches its maximum value when the step time is equal to 1. In the same time, the boundary conditions (remote displacements) are applied, with the imposed values, throughout the simulation.

6.3 Post-Processing Stage. Comparative Study

In order to validate the results and the boundary conditions applied, a checking procedure has been performed. In this way, the total load applied to the structure has to be completely balanced by the reaction forces and moments generated by the constraints described above. As input data, the material mechanical behavior considered for the analysis has been assigned to be linear elastic. This assumption has been proved valid due to the fact that the obtained maximum von Mises equivalent stress is lower than the yielding stress of the bearing material utilized (SAE 52100 or 100Cr6) equal to 1700 MPa.

In this paragraph a comparison between the three different bearing designs will be described in terms of reaction forces, von Mises equivalent stresses, and contact pressure distributions.

Taking into account the maximum load and the constraints applied to the studied model, a series of reaction forces of the most loaded row of rollers, for each bearing design, has been illustrated in Fig. 13, after retrieving Ansys post-processing data. In order to be compared, the reaction forces have been normalized considering the maximum reaction force value of 24122 WOR82A design. Fig. 13 a represents a comparison between normalized

reaction forces distribution (*Rz*) of the contact between the most loaded row of rollers and inner ring raceways of the three rolling bearings.

Because of the high angular misalignment of the application, these spherical roller bearings are able to accommodate the same load applied on the structure, but, due to different internal geometrical parameters of inner rings, the internal reaction forces distribution (*Rz*) will vary in magnitude, according to Fig. 13 a. Comparing the results of 24122 WOR82A and 24122 WOR82 designs a difference can be observed in terms of reaction forces values. That is because the bearing loads pass entirely through the raceway due to the ribless design (24122 WOR82A design), generating in this way higher normal reaction forces (*Rz*) in the contacts between rollers and inner ring raceway. Reversely, the reaction forces *Rz* of 24122 WOR82 design have lower values due to the small amount of load transmitted to the central fixed rib and due to the difference between contact angles. In order to diminish the reaction forces *Rz* and consequently the stresses, an improvement in internal geometry design of inner ring has been made by reinforcing the central fixed rib and increasing the contact angle. The normal reaction forces distribution (*Rz*) of the 24122 WOR82 and 24122 WOR82AA designs can be observed in Fig. 13 a.

Moreover, the change of inner ring contact angle brings more benefits in terms of reaction forces (*Rx*) generated in the contact between the side faces of rollers on the most loaded row and the lateral face of the central fixed rib (Fig. 13 b). Since 24122 WOR82A design has a non-integral rib design, reaction forces *Rx* are not present but are included in reaction forces *Rz*.

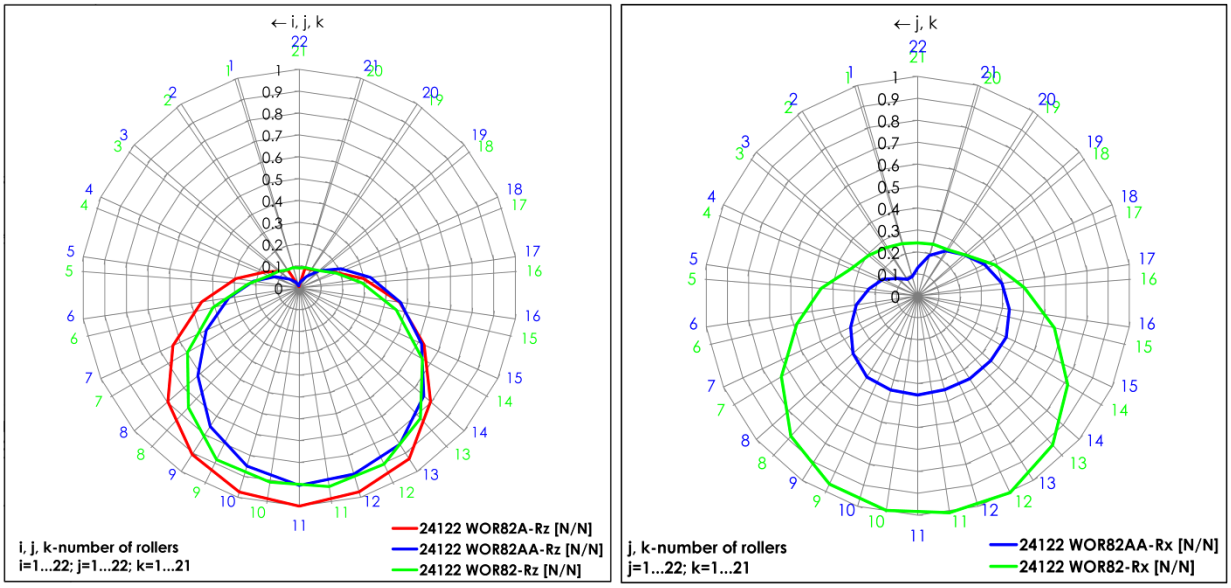

a) *b)*

Fig. 13 – Reaction force distribution graphics: a) Rz; b) Rx

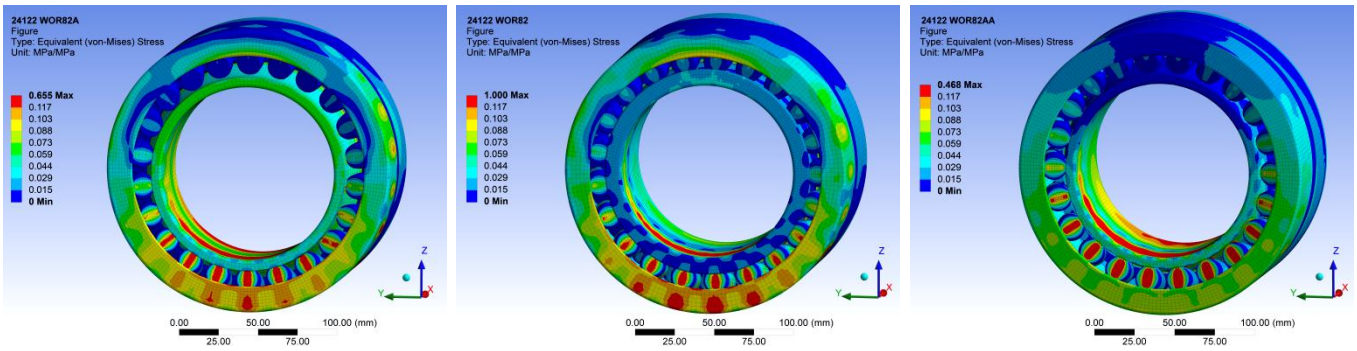

a) *b)* *c)*

Fig. 14 – Von Mises normalized equivalent stress distribution of assemblies: a) 24122 WOR82A; b) 24122 WOR82; c) 24122 WOR82AA

The general behavior of the bearings in terms of von Mises normalized equivalent stress distributions (Fig. 14) has been evaluated without taking into account the values in the shallow layers of contact areas. To correctly assess the contact pressures distribution it is necessary to assign a huge amount of finite elements to each contact zone leading to unacceptable computational time. To reduce the computational time, the NON-HERTZ software has been used to solve the contact pressures between the rollers and inner ring raceway.

Considering the reaction force distributions depicted in Fig. 13 a, b and the internal geometrical peculiarities, the bearing subjected to the highest stress is the 24122 WOR82 design, due to the fact that its *Rx* force magnitude contributes to increase the stresses inside the inner ring. By using these results as a reference, a normalization method has been applied for the three designs.

The same concept followed in case of bearing assemblies has been used also to evaluate von Mises normalized equivalent stress distributions inside the inner rings (Fig. 15). Analyzing the von Mises stress graphics related to the inner ring, it can be observed that the central fixed rib is subjected to load. 24122 WOR82AA design presents a reduced stress magnitude than 24122 WOR82. These results are confirmed by the graphic from Fig. 13 b, where the reaction forces *Rx* of the 24122 WOR82AA are significantly lower than those of 24122 WOR82.

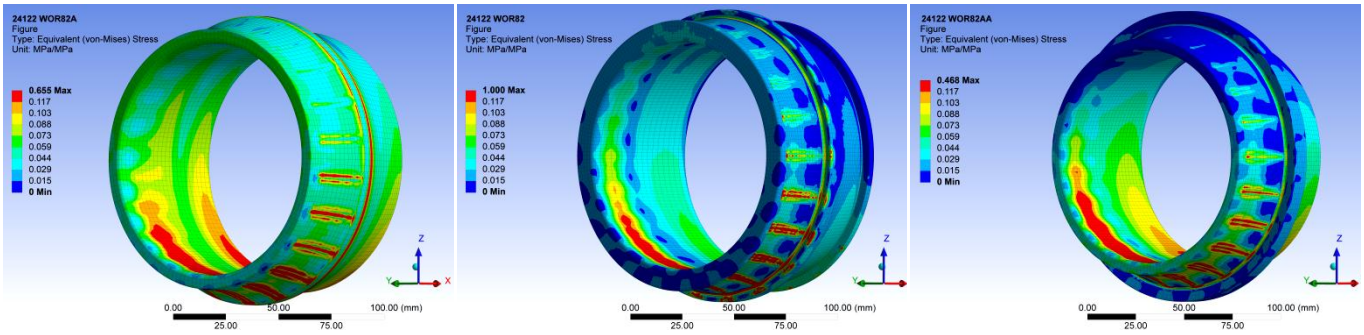

a) *b)* *c)*

Fig. 15 – Von Mises normalized equivalent stress distribution of inner rings: a) 24122 WOR82A; b) 24122 WOR82; c) 24122 WOR82AA

Regardless the magnitude of the load acting on the central fixed rib, a reduction of it is beneficial for the bearing life. A slight difference of reaction force *Rx* causes high differences in stresses inside the central fixed rib because of the undercut, which acts as a stress concentrator that increases the stress in this zone. This concept can be observed in Fig. 16, where the detailed views of the inner rings are reported. 24122 WOR82 design presents highly stressed areas in the proximity of the undercut and central fixed rib. On the contrary, in the case of 24122 WOR82AA design this effect is significantly reduced due to the contact angle modification and central fixed rib reinforcement.

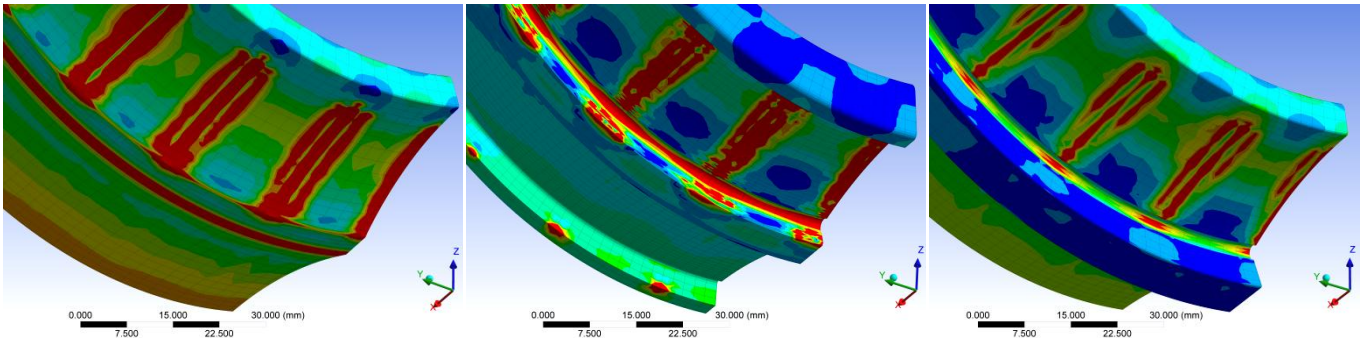

a) *b)* *c)*

Fig. 16 – Von Mises equivalent stress distribution of inner ring for: a) 24122 WOR82A; b) 24122 WOR82; c) 24122 WOR82AA

Moreover analyzing in detail the inner ring stress distributions from Fig. 17 a, the presence of edge stress concentrations on the proximity of the inner raceway edge of 24122 WOR82A design can be observed. A possible explanation of this effect is connected to the rotation of the rollers around an axis perpendicular to the main axis of the bearing, induced by the high misalignment of the mixing drum and the heavy axial load, that tend to modify the contact area between rollers and raceways. This effect is reduced in the other two designs (Fig. 17 b, c) by the central fixed rib, which guides the rollers during bearing operation. Still, high forces act on the central fixed rib of 24122 WOR82 design (Fig. 17 b), which induces, as mentioned before, undesirable stresses inside the rib. As for 24122

WOR82AA design, very low edge stresses on the inner ring raceway and a proper guidance of the rollers are ensured without causing undesired stresses inside the central fixed rib.

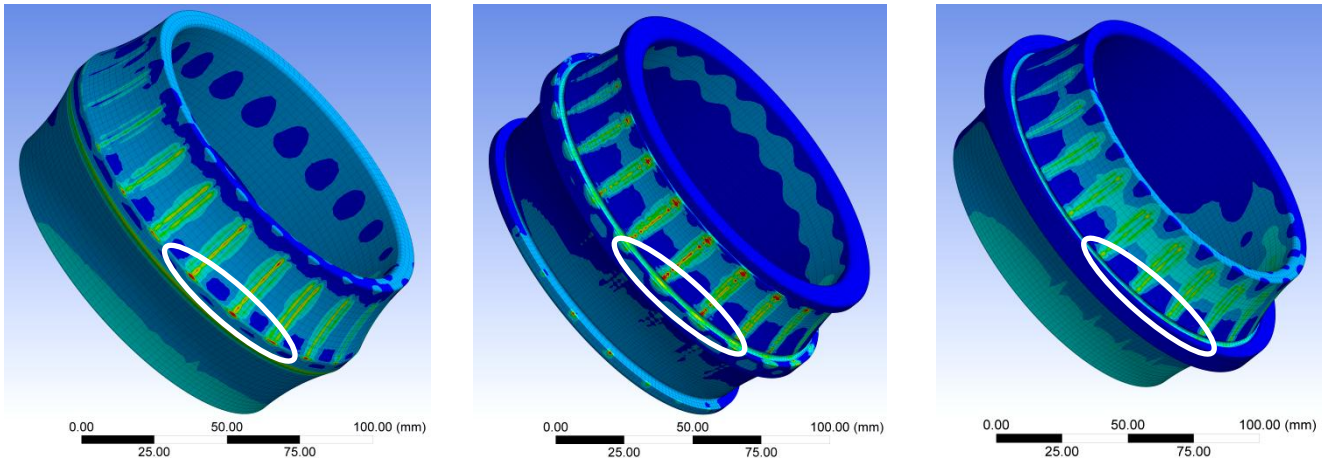

a) *b)* *c)*

Fig. 17 – Von Mises equivalent stress distribution of inner ring rib for: a) 24122 WOR82A; b) 24122 WOR82; c) 24122 WOR82AA

The normal reaction forces (*Rz*) have been used as input data for the calculation of the contact pressures between the most loaded row of rollers and inner ring raceways by using a semi-analytical method through RKB NON-HERTZ software. This numerical technique involves the conjugate gradient method (CGM) coupled with discrete convolution fast Fourier transform (DC-FFT). The efficiency of the GCM and DC-FFT algorithms in both computation time and storage, without sacrificing the accuracy of the results, has been proved by a comparison with the analytical values obtained in a Hertzian contact problem.

The pressure distributions of the three bearing designs, obtained with NON-HERTZ software, are depicted in Fig. 18. For this representation, all the contact pressure values have been normalized by using the maximum value of the most loaded roller of 24122 WOR82 with all designs. As can be seen, there is a slight difference between 24122 WOR82 and 24122 WOR82A designs in terms of contact pressures distribution, but a major difference in the upper part of the pressure distribution graphic of 24122 WOR82 design. This seems due to the different contact angle, number of rollers, both smaller in case of 24122 WOR82 design, and implicitly to the normal reaction forces (*Rz*) depicted in Fig. 13 a. On the contrary, the 24122 WOR82AA design presents a lower contact pressure distribution of all rollers compared to the other two designs. These are the results of the improved internal geometry design in terms of contact angle and central fixed rib reinforcement.

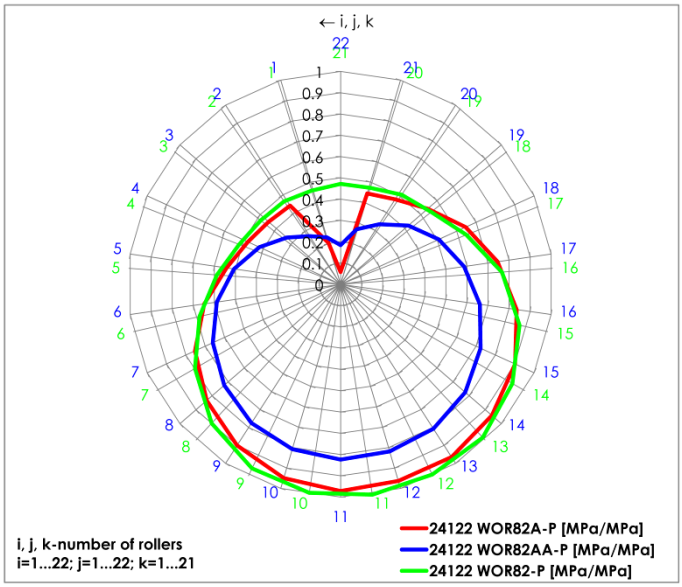

Fig. 18 – Contact pressure distributions of 24122 WOR82A, 24122 WOR82AA, and 24122 WOR82 designs

Furthermore, the maximum normalized values of contact areas (major and minor axis of the contact ellipse) and contact pressures are represented in 2D and 3D graphics (Fig. 19). Analyzing the graphics of the major and minor axis of ellipse contact area of 24122 WOR82 and 24122 WOR82AA designs, a significant difference in terms of values and shape can be noticed. This fact can be considered as an effect of the applied normal load magnitude, different radius curvature of inner ring raceway and geometry of rollers.

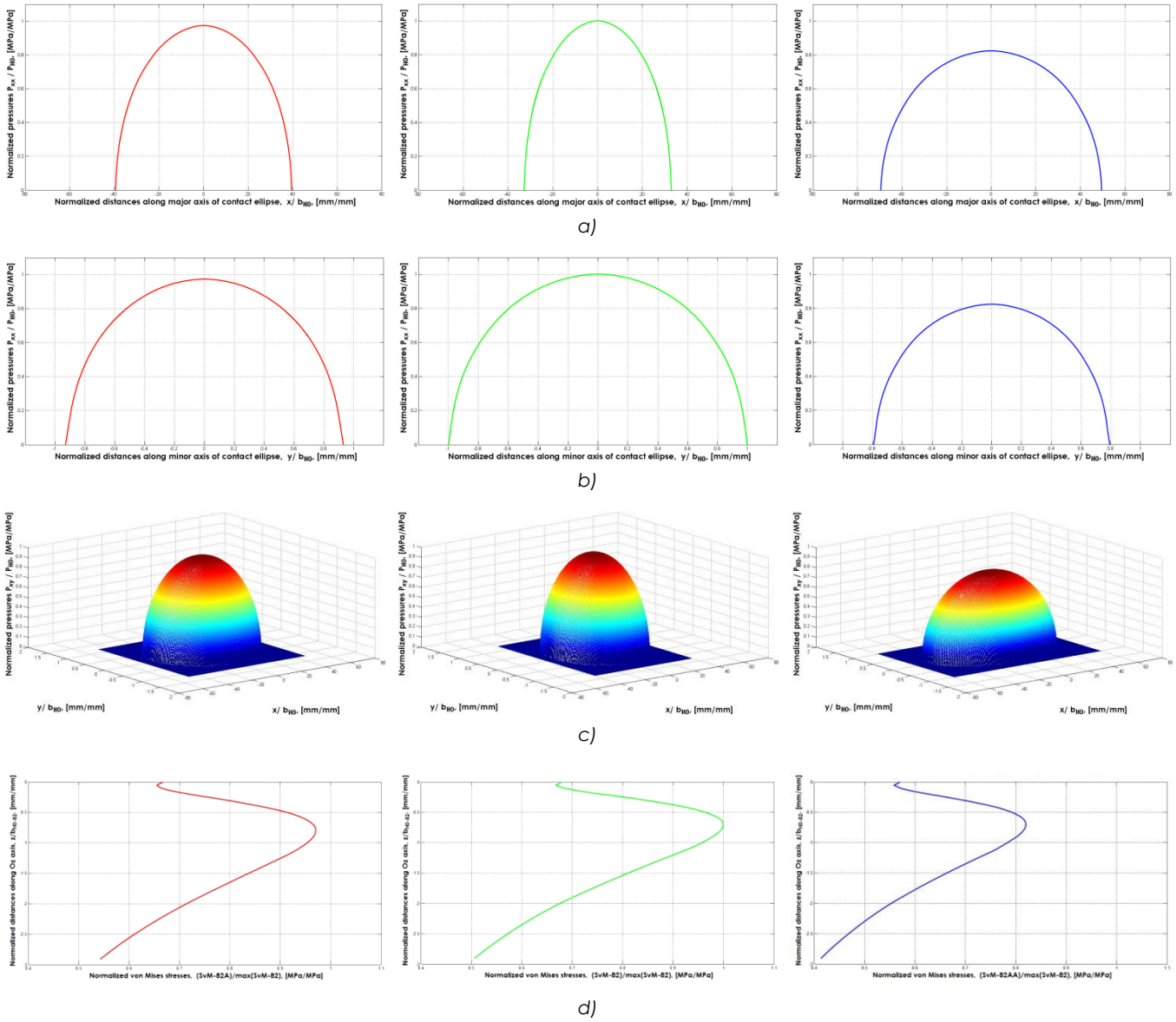

Fig. 19 – 2D ellipse contact area: a) major axis; b) minor axis; c) 3D contact pressure distributions of the most loaded rollers; d) von Mises equivalent stresses distribution in the inner ring shallow layers of 24122 WOR82A, 24122 WOR82, and 24122 WOR82AA designs

Having the pressure distribution values on the contact area of the most loaded row of rollers, the NON-HERTZ software has been further involved in obtaining the depth distributions, inside the shallow layer, of all six components of the stress tensor and finally the depth distribution of von Mises equivalent stresses of all three inner ring designs (Fig. 20 d). The components of the stress tensor, induced by the entire pressure over the contact area, in a generic point *M(x, y, z)* are obtained by superposition and using the convolution products:

$$\sigma_{ij}(x,y,z) = \sum_{k=0}^{N_x-1} \sum_{l=0}^{N_y-1} (C_{ijkl} \cdot p_{kl}) \quad (1)$$

where the influence function $C_{ijkl}(x, y, z)$ describes the stress component $\sigma_{ij}(x, y, z)$ due to a unit pressure acting in patch (k, l). This is a Neumann type problem of the elastic half-space theory. Based on stress tensor components the von Mises equivalent stress can be obtained using its definition:

$$\sigma_{eq} = \sqrt{\frac{1}{2}\left[(\sigma_{xx} - \sigma_{yy})^2 + (\sigma_{yy} - \sigma_{zz})^2 + (\sigma_{zz} - \sigma_{xx})^2 + 6(\tau_{xy}^2 + \tau_{yz}^2 + \tau_{zx}^2)\right]} \quad (2)$$

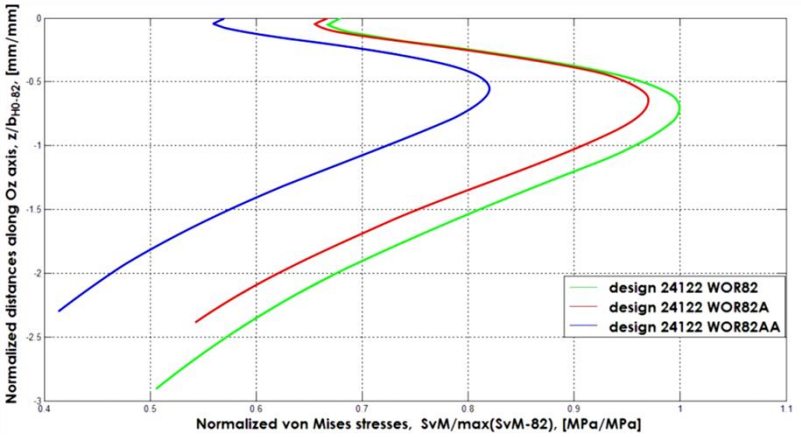

Fig. 20 – Von Mises equivalent stresses distribution in the inner ring shallow layers of 24122 WOR82A, 24122 WOR82, and 24122 WOR82AA designs

Fig. 20 reveals significant differences in terms of von Mises equivalent stress magnitude through the whole inner ring thickness between 24122 WOR82AA and the other two designs. It is evident that the geometrical characteristics and contact pressures distribution of 24122 WOR82AA design result in a lower equivalent stress, thus leading to a better overall performance of the bearing.

7 CONCLUSIONS

Examining the concrete mixer gearbox technical requirements, the RKB Group has studied its most critical component, the main spherical roller bearing, in three different designs. After evaluating the results, the best solution for this project has been found by the RKB Technical Department in SRB 24122 WOR82AA design, which succeeds in accomplishing all of the application operating conditions. Among other things, this special bearing type has been optimized to sustain additional loads and friction at low operating speeds (max 20 rpm), increase permissible misalignment up to ±6° and ensure a longer rating life.